Jin Jin, Yan (Orcid ID: 0000-0002-3627-0323)
Ramakrishnan Vidya (Orcid ID: 0000-0001-7726-6278)

Quantitative Systems Pharmacology Model of the Amyloid Pathway in Alzheimer's Disease: Insights into the Therapeutic Mechanisms of Clinical Candidates

Vidya Ramakrishnan[1], Christina Friedrich[2], Colleen Witt[2], Robert Sheehan[2], Meghan Pryor[2], Jasvinder K. Atwal[1], Kristin Wildsmith[1], Katherine Kudrycki[2], Seung-Hye Lee[1], Norman Mazer[4], Carsten Hofmann[4], Reina N. Fuji[1], Jin Y. Jin[1], Saroja Ramanujan[1], Michael Dolton[3], Angelica Quartino[1]

[1]Genentech, Inc., South San Francisco, CA, USA
[2]Rosa & Co., LLC., San Carlos, CA, USA
[3]Roche Products Australia Pty Ltd, Sydney, Australia
[4]F. Hoffmann-La Roche Ltd, Basel, Switzerland

Corresponding author: Vidya Ramakrishnan
Address: Genentech, Inc., South San Francisco, CA, USA
Phone: +1 (650) 225-6154 (Office)
E-mail: ramakrishnan.vidya@gene.com

This article has been accepted for publication and undergone full peer review but has not been through the copyediting, typesetting, pagination and proofreading process which may lead to differences between this version and the Version of Record. Please cite this article as doi: 10.1002/psp4.12876

Conflict of Interest Statements (Each author must disclose and describe any involvement, financial or otherwise, that might potentially bias his or her work)**:**

Vidya Ramakrishnan, Jasvinder Atwal, Seung-Hye Lee, Reina Fuji, Saroja Ramanujan, and Jin Y. Jin are full-time employees of Genentech, Inc. and may own company stock/stock options.

Christina Friedrich, Colleen Witt, Robert Sheehan, and Katherine Kudrycki are current employees of Rosa & Co. LLC and may own company stock/stock options.

Meghan Pryor is a former full-time employee of Rosa & Co. LLC.

Michael Dolton is a former full-time employee of Genentech, Inc. and is a current full-time employee of Roche Products Australia Pty Ltd and may own company stock/stock options.

Norman Mazer and Carsten Hofmann are current employees of F. Hoffmann-La Roche Ltd and may own company stock/stock options.

Angelica Quartino and Kristin Wildsmith are former full-time employees of Genentech, Inc.

Funding information:
This analysis was funded by Genentech, Inc. South San Francisco, CA, USA.

Keywords: Alzheimer's disease, QSP, *APOE ε4*, amyloid beta, solanezumab, crenezumab, aducanumab, gantenerumab

Abstract (247 of 250-word limit):

Despite considerable investment into potential therapeutic approaches for Alzheimer's disease (AD), currently approved treatment options are limited. Predictive modeling using quantitative systems pharmacology (QSP) can be used to guide the design of clinical trials in AD. This study developed a QSP model representing beta-amyloid (Aβ) pathophysiology in AD. The model included mechanisms of Aβ monomer production and aggregation to form insoluble fibrils and plaques; the transport of soluble species between the compartments of brain, cerebrospinal fluid (CSF), and plasma; and the pharmacokinetics, transport, and binding of monoclonal antibodies to targets in the 3 compartments. Ordinary differential equations were used to describe these processes quantitatively. The model components were calibrated to data from the literature and internal studies, including quantitative data supporting the underlying AD biology and clinical data from clinical trials for anti-Aβ monoclonal antibodies aducanumab, crenezumab, gantenerumab, and solanezumab. The model was developed for an apolipoprotein E (*APOE*) *ε4* allele carrier and tested for an *APOE ε4* non-carrier. Results indicate that the model is consistent with data on clinical Aβ accumulation in untreated individuals and those treated with monoclonal antibodies, capturing increases in Aβ load accurately. This model may be employed to investigate additional AD mechanisms and their impact on biomarkers, as well as predict Aβ load at different dose levels for monoclonal antibodies with known targets and binding affinities. This model may facilitate the design of scientifically enriched and efficient clinical trials by enabling *a priori* prediction of biomarker dynamics in the brain and CSF.

INTRODUCTION

Alzheimer's disease (AD) is a chronic and progressive neurodegenerative disease associated with decline in memory and cognitive function in patients.[1] Current estimates suggest that between 15% and 20% of people above the age of 60 have mild cognitive impairment, and up to 15% of these patients will progress to dementia within a year.[2] The projected worldwide burden of AD could be over 100 million by 2050. The known pathophysiology of AD includes the aggregation and accumulation of amyloid beta (Aβ) into oligomers and plaques, and the aggregation of the microtubule-associated protein tau into neurofibrillary tangles in the brain.[1] Both Aβ and tau are biomarkers for AD diagnosis and have been targets for drug development.[3]

Despite considerable investment, currently, 4 drugs are approved by the Food and Drug Administration (FDA) to treat symptoms of AD; however, they do not halt or significantly slow disease progression, with over 100 having negative results in clinical trials.[1, 4] In June 2021, the FDA granted accelerated approval to aducanumab, a monoclonal antibody (mAb) targeting Aβ, as the first disease-modifying therapeutic for the treatment of AD based on reduction of Aβ plaque in the brain and the reasonable likelihood to predict a clinical benefit.[5] Aducanumab was the first drug approved for AD since 2003.[5]

Clinical trials in AD have been facing setbacks due to a lack of effect on the primary and secondary clinical endpoints that assess cognitive and functional progression in patients.[4] Numerous challenges contribute to this lack of therapeutic progress in the field. Large sample sizes are required for AD trials due to the heterogeneous responses observed in participants.[6] Issues with participant drop-out or death can be a problem due to the long duration of trials

needed to evaluate cognitive improvements adequately.[6] Dose-ranging studies are not easily feasible, and failed trials lead to questions about drug dosing and efficacy.[7] The right choice of clinical trial participants is a factor in clinical trial success as well. Considering AD pathologic manifestation begins much earlier than symptom onset, a key challenge in early stages of the disease is identification of participants who could benefit from treatment.[6]

Biomarkers can play a key role in clinical trial success too. The accelerated approval of aducanumab was based on the drug's effect on the surrogate biomarker endpoints of dose- and time-dependent reduction in the level of amyloid plaque in the brain.[5] This emphasizes the considerable role that biomarkers can play in closing the gap between drug effect and potential clinical benefit. Identifying the mechanisms of disease progression and drug effect in the brain via non-invasive, easy-to-measure, blood-based biomarkers would be ideal. Better methods to assess adequate concentrations of the drug available in the brain are also needed.

Predictive modeling provides one approach to support drug development in the face of these issues. Quantitative systems pharmacology (QSP) modeling aims to quantitatively assess drug pharmacology and downstream biology, including disease pathophysiology, in tandem.[8] Given the biological complexity of AD, QSP modeling is well suited for applications to guide clinical drug development. QSP modeling enables target identification and benchmarking of similarities and differences in dynamics of Aβ or tau biomarkers at different states of aggregation. It allows for representation of virtual patients based on targeted biological elements and enables simulation of clinical trial scenarios. *A priori* predictions of biomarker dynamics in difficult to measure regions, such as the brain and cerebrospinal fluid (CSF), can be made. QSP also provides a model to test various target- and treatment-related hypotheses,

leading to insights and guidance for drug development. More recently QSP models representing Aβ dynamics in AD have been published in the literature and highlight the strength of the approach to understand disease progression and Aβ biomarker dynamics in AD.[9, 10] Our work is uniquely distinguished from the prior work on two key aspects: a) this work characterizes the dynamics of different biomarker species (Aβ 40 and 42 specifically) in detail. This enables a biologically plausible hypothesis-driven approach to understand the differences in the mode of action of the mAbs targeting the Aβ pathway thereby enabling quantitative benchmarking; b) the work incorporates and enables evaluation of the mechanistic differences based on the stage of the disease and the APOE ε4 carrier status enabling future exploration based on virtual patients with a specific phenotype.

Here we present the development of a QSP model for AD and investigate its predictive capability using data from clinical trials of novel therapeutic agents targeting aggregated Aβ. The current model is solely focused on the Aβ component of AD pathology, considering Aβ pathology precedes tau pathology and cognitive impairment,[11] without incorporating tau pathology or cognitive functionality. Our goal is to create a model that can support the development of clinical trials by allowing researchers to predict Aβ dynamics in the brain prior to participant enrollment.

METHODS

The AD QSP model was developed as a set of ordinary differential equations (ODEs; available in the supplemental material) implemented in MATLAB®SimBiology® version 2017B. The ODEs represent key pathophysiologic and therapeutic pathways in 3 compartments: the

brain, CSF, and plasma (**Figure 1** depicts a schematic overview). The model tracks the insoluble and soluble biomarkers across these compartments, including production of Aβ in the brain and plasma, aggregation of Aβ in the brain, and the transport of soluble Aβ from the brain to the CSF and plasma. Aβ monomer production and secretion is regulated by β-secretase 1 (BACE1) and γ-secretase.[12] Aβ40 and Aβ42 are produced and tracked separately and exhibit different behaviors, including higher aggregation and slower clearance rates for Aβ42.[13, 14]

The temporal scope of the model focuses on the ~20-year progression duration during which Aβ aggregation in the brain exhibits constant linear growth, i.e., the upward slope of the characteristic S curve.[11] Aggregation is modeled as progressing from monomers to oligomers (assumed to be 10-mers) to fibrils to plaque. Aβ42 monomers aggregate at a higher rate than Aβ40, forming oligomers that contain a mix of species with relatively more Aβ42 than Aβ40.[15] Once the aggregated species have formed, their Aβ42 and Aβ40 content is not tracked separately, and further aggregation to higher order species is assumed to be driven by the species that form them. To facilitate comparison to clinical data, the quantitative assessment of the total Aβ burden, measured clinically as the standard uptake value ratio (SUVR) from positron emission tomography (PET) imaging, is calculated in the model assuming a linearly proportional relationship between the insoluble Aβ (fibril plus plaque) mass and SUVR. Soluble Aβ species are transported across the blood–brain-barrier by active transport or from brain interstitial fluid to CSF by bulk flow. Aβ monomers are also produced peripherally. All Aβ production, aggregation, transport, and clearance process parameters were informed by mechanistic data (**Table 1**).[16–26]

States of Aβ aggregation in the three compartments were calibrated simultaneously to match available clinical data for untreated participants and participants undergoing treatment with the Aβ-targeting mAbs solanezumab,[27] crenezumab,[26] aducanumab,[28] and gantenerumab.[21, 29] Aβ-targeting mAbs in the model can be configured to bind to any form of Aβ including monomers, oligomers, fibrils, and plaque. The binding affinity for each form is mAb-specific, with solanezumab binding strongly to monomers only; crenezumab binding strongly to oligomers, moderately to monomers, and weakly to fibrils, and plaques; and

aducanumab and gantenerumab binding strongly to fibrils, plaque, and oligomers, and weakly to monomers (**Table 2**).[28, 30–33]

Following subcutaneous or intravenous dosing with a mAb, the model follows mAb transport into the CSF and brain via passive diffusion. The pharmacokinetics of the mAb is described by a target-mediated drug disposition model based on its binding to Aβ. It then predicts brain target engagement based on target concentrations, mAb concentrations, and mAb binding properties for Aβ monomers, oligomers, and fibrils/plaque. Once bound to a target, the mAbs are assumed to inhibit further aggregation. The implementation of aducanumab and gantenerumab required an additional assumption of microglial activation and clearance of plaque, as further discussed in the results below. For more specific details about model calibration and implementation, see the supplemental methods.

QSP modeling is useful for investigating the system-level effects of mechanistic differences between drugs or patient variability. One well-documented difference between patients with AD is in the apolipoprotein E (*APOE)* gene.[34] To date, *APOE* remains the gene with the strongest impact on risk in non-familial sporadic AD.[34] In addition to its role in lipid metabolism,[35] APOE also mediates active transport of Aβ across the blood–brain barrier[36] and regulates Aβ uptake into astrocytes.[37] The *APOE* gene is polymorphic, with three major alleles that encode three protein isoforms: epsilon 2 (APOE ε2), epsilon 3 (APOE ε3), and epsilon 4 (APOE ε4).[35] The ε4 isoform is associated with increased risk of AD, while ε2 appears to be protective and ε3 is considered 'neutral'. The impact of *APOE ε4* expression on rates of Aβ production and clearance have been reported in the literature.[38, 39]

The model was initially developed to represent the most typical patient with AD, an *APOE ε4* carrier.[1] As a way of validating the QSP model's representation of biology, we tested whether implementing observed differences between carriers and non-carriers in the model would produce the differences in Aβ aggregation rates that have been observed. Toward this goal, a second virtual patient was created that represented an *APOE ε4* non-carrier. Mechanistic differences between *APOE ε4* carriers and non-carriers have been identified and implemented as parameter differences in the model as summarized in **Table 3**.[38, 39]

RESULTS

The AD model integrates known characteristics of AD into a single mechanistic framework. Aβ species concentrations in brain, CSF, and plasma are consistent with data and are dynamically maintained. Aβ plaque in the brain increases at a rate that is consistent with clinical progression data. The model is also able to reproduce clinical responses to Aβ-targeting antibodies, as further described below. Only parameters relevant to mAb treatment, such as binding rates for different Aβ species, were changed to produce appropriate responses to all treatments.

Pharmacokinetics

Prior pharmacokinetic (PK) models were adapted into the QSP model to recapitulate the dynamics of mAb concentrations in the plasma, and CSF. The mAb transport across the compartments was described using first-order processes. A peripheral compartment was included to capture the distribution of the mAb to other compartments. The model described

the plasma PK of the different mAbs at varied dosing-ranges and dosing-frequencies well. The calibration results are represented in **Figure 2A-C** and **Figure S1A**.

Clinical trial data from Phase II and Phase III studies of crenezumab were used for calibration of the CSF PK. The model described the data, which suggested that the CSF steady-state mAb concentrations are generally between 0.2% and 0.3% of plasma concentration.[40, 41] The calibrated model was used to simulate the CSF and brain PK of other mAbs (**Figure 2D-F and Figure S1B**).

Pharmacodynamic biomarkers

Plasma and CSF

The half-life of Aβ in plasma is approximately 3 hours.[42] It was estimated that 40% of Aβ in plasma was derived from effluxed Aβ from the brain[43] and the remainder was produced in the periphery. Calibration of plasma Aβ with mAb treatment using the crenezumab studies produced a model that adequately characterizes the biomarker dynamics of soluble Aβ40 and Aβ42 in plasma for crenezumab (**Figure 2G and Figure S1C**).

The predominant mechanism of Aβ clearance in the CSF was implemented as efflux to plasma. It has been shown that enzymatic degradation activity is present in CSF but is greatly reduced in prodromal AD.[44] Therefore, we assumed that the contribution to clearance via enzymatic degradation was negligible as compared with efflux. The reported absolute concentrations of Aβ in CSF are highly variable[40] and hence the data calibration was performed using percent changes in the levels of the soluble biomarkers (**Figure 2H and Figure S1D**). The

model was used to predict the percent change in Aβ in CSF with solanezumab treatment and the predictions are consistent with the data (**Figure 2I**).

Brain predictions

The model was used to simulate and benchmark the effect of mAb administration on the dynamics of Aβ states in the brain (**Figure 2J-L**). The simulations were in accordance with the relative specificities of the mAbs for the various Aβ aggregation states and the predicted consequences of target engagement on state dynamics. The model suggests that the plaque-targeting antibodies, gantenerumab and aducanumab, reduce plaque in the brain to below 10% of the initial concentrations by the end of the treatment duration (**Figure 2L**; dose and duration based on Phase III clinical trials). As Aβ plaque reduces, the oligomeric Aβ species also reduce as a consequence (**Figure 2K**). Consistent with clinical data, the model indicates that crenezumab, which primarily targets the oligomeric state, reduces the oligomeric Aβ and slows plaque growth (**Figure 2K**), but has minimal effect on existing Aβ plaque burden (**Figure 2L**). The Aβ monomer-targeting antibody solanezumab binds the monomeric state and simulations show no effect on oligomers or plaque at its clinical dose.

PET imaging

The calibration of PET imaging-based biomarker data included florbetapir SUVR data from crenezumab Phase III CREAD (NCT02670083) and CREAD2 (NCT03114657) trials, and the aducanumab Phase I trial (NCT01677572).[28] The data from these studies represented SUVR change from baseline. The model calibrations are shown in **Figure 3**. According to the model,

crenezumab (**Figure 3B**) inhibits nascent plaque formation but does not produce a significant decrease in total plaque. Aducanumab produces a dose-dependent decrease in total plaque (**Figure 3A**). The model slightly under predicts the early reduction in SUVR but captures the response at a later time point.

The calibrated model was then used to predict the SUVR change from baseline upon administration of the Phase III titration dose of aducanumab. The model predictions qualitatively capture the observed data from the Phase III studies (EMERGE: NCT02484547) as seen visually in **Figure 3C**. Similarly, the model was also used to predict the percent change in Aβ burden with gantenerumab treatment. The decrease in insoluble Aβ states compared well with the reported decrease in absolute Centiloids.[29]

Investigation of plaque clearance by plaque-binding immunoglobulin G1 (IgG1) antibodies

The mechanism of plaque clearance is a key element in evaluating and predicting mAb treatment efficacy. In the model, it is assumed that endogenous plaque clearance in absence of treatment is negligible. However, mAb binding to plaque allows for the recruitment and activation of microglia, which are capable of clearing plaque. The model implementation of the plaque-binding mAbs aducanumab and gantenerumab assumed that microglia would clear sections of plaque directly bound to the mAb via phagocytosis following a direct interaction between the bound mAb and fragment crystallizable (Fc) receptors. However, initial model simulations did not agree with published data following aducanumab treatment (**Figure S2**). Aducanumab treatment resulted in a fast initial clearance of plaque during the first year of

treatment which began to level off during the second year.[28, 45] Model simulations suggested that the reported level of plaque clearance could not be achieved by the presumed mechanism of clearing only antibody-bound plaque. Given the estimated concentration of mAb in the brain and the known binding affinity of the mAb, only a small amount of plaque would be bound to the mAb at a given time. This assumption would lead to linear rather than exponential clearance dynamics, as demonstrated in initial simulations. Varying the clearance rate for mAb bound to plaque did not eliminate this discrepancy as the model could match either the 1-year data point or the 2-year data point, but not both.

The rate of plaque clearance following aducanumab treatment appears to suggest first-order clearance of all plaque (**Figure 3A**). This effect is consistent across multiple doses of the drug and cannot be achieved under the assumption that only plaque directly bound to the mAb is being cleared by the newly activated microglia. To account for the discrepancy between the simulations and data, a new term was added to incorporate microglia activation in the presence of therapeutic antibodies. This effect is more pronounced in IgG1 antibodies, which are known to be relatively more activating compared with other IgG isotypes.[46] Once microglia were activated in the model, the microglia were capable of clearing any plaque, independent of specific mAb binding. This mechanism still results in a small lag in achieving the ultimate clearance rate until mAb levels in the brain reach steady state, but the final result is a first-order clearance of all plaque. Updated simulations qualitatively describe the clinical data for plaque clearance following treatment with IgG1 antibodies, such as aducanumab (**Figure 3A**).

Creation of an APOE ε4 non-carrier virtual patient

The *APOE ε4* non-carrier virtual patient was developed by implementing mechanistic differences between *APOE ε4* carriers and non-carriers (**Table 3**).[38, 39] Decreased Aβ42 production and increased clearance in the *APOE ε4* non-carrier compared with the carrier caused a decrease in the Aβ42:40 ratio, decreased aggregation rate, and slower plaque progression (SUVR; **Figure 4**) for the *APOE ε4* non-carrier in the model, consistent with clinical reports of earlier amyloid deposition in *APOE ε4* carriers.[47] The model's prediction of the appropriately reduced progression rate in the non-carrier as a result of the mechanistic differences between carriers and non-carriers was a useful validation that plaque progression mechanisms are appropriately captured in the model.

Discussion

A major value of employing QSP to research a complex process, such as the pathology that underlies AD, is the ability to query the collective effects on the system that arise from numerous mechanistic factors acting in concert. We used QSP modeling to simulate Aβ dynamics in AD patients. The model was calibrated using virtual patients experiencing Aβ progression who possess the *APOE ε4* gene. We introduced treatment effect using 4 Aβ targeting mAbs to calibrate/assess change in Aβ in the brain, CSF, and plasma. The model was then tested using virtual patients who did not have the *APOE ε4* gene. The model was able to recapitulate untreated and treated outcomes and biomarker dynamics.

The results of the brain prediction analysis confirmed that the target states, binding affinity, and the antibody concentrations determine biomarker dynamics. The model can be leveraged to predict Aβ burden or SUVR at different dose levels for mAbs with different binding specificities. The profile of the mAb's binding properties and unique specificities for Aβ states

(i.e., monomer vs oligomer vs plaque) can lead to potentially different mechanisms of action with varied outcomes in both *APOE* subpopulations.

The brain PK simulations for plaque-targeting mAbs suggested that steady-state PK concentrations are achieved only when plaque and mAb binding reach an equilibrium, due to the presence of large amounts of accumulated plaque in the AD brain that acts as a sink for mAb binding. This process takes time due to the excess of plaque relative to mAb concentration in the brain at the beginning. The time taken to achieve this equilibrium is dependent on the dose administered with higher doses reaching equilibrium sooner than lower doses. At the clinical doses, the model simulations suggest that aducanumab binding aggregated Aβ takes about 4–5 times longer to achieve equilibrium in contrast to crenezumab binding to oligomers.

Modeling of PET imaging biomarker data suggested that clearance of plaque is not proportional to mAb-bound plaque alone. Modeling indicated that the clearance of unbound plaque is necessary to explain the observed clinical decrease in SUVR following aducanumab and gantenerumab treatment. This is supported by biological evidence for microglial activation by plaque-targeting antibodies. There are a number of potential hypotheses to explain how mAb in the brain leads to a decrease in plaque burden. There is strong evidence that the isotype backbone of the mAb influences the strength of the glial response to treatment.[48] Both aducanumab and gantenerumab are IgG1 antibodies, which compared with other isotypes, are known to bind Fc receptors with higher affinity and elicit more robust activation of microglia and other innate immune cells. Therefore, clearance of plaque by microglia-mediated phagocytosis would be more efficient with treatments that employ antibodies of the IgG1 isotype. Indeed, this appears to be supported by the observation that high doses of both

aducanumab and gantenerumab in clinical trials were associated with a significant risk of amyloid-related imaging abnormalities, believed to be a consequence of high glial activation.[49] A more detailed and mechanistic representation of microglia should be capable of producing an even greater match to the data, as modeling an initial burst of activation and recruitment of microglia following brain penetration by the mAb could explain the strong initial response as mAb levels are still reaching equilibrium. This lack of detail is a current limitation of the model and highlights a potential opportunity to further expand the model to include microglial activation mechanisms.

APOE ε4 carriers and non-carriers can have different responses to therapeutic treatments as well.[50] Implementation of mechanistic differences between *APOE ε4* carriers and non-carriers led to a greater Aβ aggregation in carriers than non-carriers, providing an important validation for the model. Our simulation results indicate that the model may be leveraged to predict potential differences in carrier vs non-carrier progression of Aβ accumulation and a subsequent effect on response to therapeutic treatments, especially on their amyloid lowering capabilities.

The current model has been used to compare and benchmark Aβ targeting therapies and suggests that agents targeting insoluble forms, specifically fibrils and plaque, are more effective in reducing the Aβ burden in the brain in comparison to therapies that primarily target soluble forms of Aβ (monomers and oligomers). The binding affinity to the diverse Aβ species can determine the relative clearance of the different forms of Aβ. However, the activation of downstream processes as a consequence of binding and clearance of Aβ also play a major role in the totality of effect on Aβ burden. It is imperative to understand the downstream effect of

Aβ engagement to understand its effects on Aβ clearance and further on the efficacy markers, cognition, and function. This model lays a foundation to explore similar downstream processes. The model is a useful platform for hypothesis testing of newer therapies targeting the Aβ pathway, or for assessing the impact of improved brain uptake technologies, and is positioned to leverage incoming data from very recent Aβ targeting agents such as donanemab and lecanemab, not used in model development, to improve the model calibration and predictions.

A key feature of the QSP model is its flexibility to include additional mechanisms and pathways to the structure. This can be implemented in 2 ways: including diverse additional pathways (e.g., tau pathway) with the known connections of these pathways to the Aβ pathway and extending mechanistic details to already existent pathways (e.g., microglial plaque clearance and endogenous plaque clearance). In addition to the *APOE ε4* non-carrier virtual population example, other extensions of the virtual population could include representation of autosomal-dominant AD patients, more progressed moderate AD patients, and more. The model serves as a backbone to implement and evaluate several such disease mechanisms and their potential impact on biomarker dynamics.

The model facilitates the design of more informative and efficient clinical trials by enabling *a priori* prediction of biomarker dynamics and target engagement in the brain **(Figure 2J-L)**. Model validation extends the value of the model beyond that of a predictive tool. Our results show that mechanistic models can be used to examine the systemic implications of mechanistic perturbations and diversity more generally. The manifestation of pathology is rarely the result of a single factor, but rather the collective result of many factors working in concert. For example, *APOE ε4* non-carrier simulations that matched observation were

achieved by implementing numerous contributing factors simultaneously. QSP modeling allows the query into emergent behaviors that are simply not manifested when the components are reduced in isolation. Our work illustrates that a systems approach can reveal insights that may otherwise be unrealized when employing reductionist approaches alone.

Study Highlights (150 of 150-word limit [not including the questions, 31 words]):

What is the current knowledge on the topic?

Designing clinical trials for Alzheimer's disease (AD) is challenging. Quantitative systems pharmacology modeling supports the design of scientifically informed clinical trials.

What question did this study address?

How to leverage the data from prior clinical studies and known pathophysiology of AD quantitatively to understand disease and biomarker dynamics.

What does this study add to our knowledge?

The model enables simulation of target engagement and biomarker dynamics upon treatment. The study confirmed that documented mechanistic differences between apolipoprotein E *ε4* carriers and non-carriers can account for their different amyloid plaque progression rates. The study demonstrated that clearance of antibody-bound plaque is not sufficient to account for the clinical efficacy of aducanumab and suggested a hypothesized mechanism of plaque clearance due to microglial activation that is scientifically grounded and dynamically consistent with clinical results.

How might this change drug discovery, development, and/or therapeutics?

The model provides a platform to test competing mechanisms targeting the Aβ pathway and alternative biological mechanisms to assess the impact on biomarkers providing *a priori* information to design efficient clinical studies.

Acknowledgments

Medical writing support was provided by Heather Taft, PhD, and Sarah Engelberth, PhD, of Medical Expressions (Chicago, IL), funded by F. Hoffmann-La Roche.

Author contributions

V.R., C.F., C.W., R.S., M.P., J.A., K.W., K.K., S-H.L., N.M., C.H., R.N.F., J.Y.J., S.R., M.D., and A.Q. wrote the manuscript. V.R., C.F., C.W., R.S., M.P., J.A., K.W., K.K., S-H.L., N.M., C.H., R.N.F., J.Y.J., S.R., M.D., and A.Q. designed the research. V.R., C.F., C.W., R.S., M.P., and K.K. performed the research. V.R., C.F., C.W., R.S., M.P., J.A., K.W., K.K., S-H.L., N.M., M.D., and A.Q. analyzed the data. V.R., C.F., C.W., R.S., M.P., J.A., K.W., K.K. S-H.L., N.M., M.D., and A.Q. contributed new reagents/analytical tools.

References

1. Alzheimer's Association. 2021 Alzheimer's disease facts and figures. *Alzheimers Dement*. **17**, 327– 406 (2021).

2. Petersen, R.C. Mild Cognitive Impairment. *Continuum (Minneap Minn)*. **22**, 404– 418 (2016).

3. Huang, L.-K., Chao, S.-P. & Hu, C.-J. Clinical trials of new drugs for Alzheimer disease. *J. Biomed. Sci*. **27**, 18 (2020).

4. Mehta, D., Jackson, R., Paul, G., Shi, J. & Sabbagh, M. Why do trials for Alzheimer's disease drugs keep failing? A discontinued drug perspective for 2010–2015. *Expert Opin. Investig. Drugs* **26**, 735– 739 (2017).

5. FDA. FDA Grants Accelerated Approval for Alzheimer's Drug. https://www.fda.gov/news-events/press-announcements/fda-grants-accelerated-approval-alzheimers-drug. Accessed January 18, 2022.

6. Brookmeyer, R. & Abdalla, N. Design and sample size considerations for Alzheimer's disease prevention trials using multistate models. *Clin. Trials* **16**, 111– 119 (2019).

7. Bretz, F., Dette, H. & Pinheiro, J.C. Practical considerations for optimal designs in clinical dose finding studies. *Stat. Med*. **29**, 731– 742 (2010).

8. Musante, C.J., Ramanujan, S., Schmidt, B.J., Ghobrial, O.G., Lu, J. & Heatherington, A.C. Quantitative Systems Pharmacology: A Case for Disease Models. *Clin. Pharmacol. Ther*. **101**, 24– 27 (2017).

9. Karelina, T., *et al*. Studying the progression of amyloid pathology and its therapy using translational longitudinal model of accumulation and distribution amyloid beta. *CPT Pharmacometrics Syst Pharmacol*. **6**, 676– 685 (2017).

10. Madrasi, K., *et al*. Systematic in silico analysis of clinically tested drugs for reducing amyloid-beta plaque accumulation in Alzheimer's disease. *Alzheimers Dement*. **17**, 1487– 1498 (2021).

11. Jack, C.R., Jr., *et al*. Tracking pathophysiological processes in Alzheimer's disease: An updated hypothetical model of dynamic biomarkers. *Lancet Neurol*. **12**, 207– 216 (2013).

12. Schenk, D., Basi, G.S. & Pangalos, M.N. Treatment strategies targeting amyloid β-protein. *Cold Spring Harb. Perspect. Med*. **2**, a006387 (2012).

13. Deane, R.*, et al*. LRP/Amyloid β-Peptide Interaction Mediates Differential Brain Efflux of Aβ Isoforms. *Neuron*. **43**, 333– 344 (2004).

14. Garai, K. & Frieden C. Quantitative analysis of the time course of Aβ oligomerization and subsequent growth steps using tetramethylrhodamine-labeled Aβ. *Proc. Natl. Acad. Sci. USA*. **110**, 3321– 3326 (2013).

15. Roberts, B.R., *et al*. Biochemically-defined pools of amyloid-β in sporadic Alzheimer's disease: correlation with amyloid PET. *Brain* **140**, 1486– 1498 (2017).

16. Shaw, L.M., *et al*. Cerebrospinal fluid biomarker signature in Alzheimer's disease neuroimaging initiative subjects. *Ann. Neurol*. **65**, 403– 413 (2009).

17. Mehta, P.D.*,* Pirttilä, T., Mehta, S.P., Sersen, E.A., Aisen, P.S. & Wisniewski, H.M. Plasma and cerebrospinal fluid levels of amyloid beta proteins 1-40 and 1-42 in Alzheimer disease. *Arch. Neurol*. **57**, 100– 105 (2000).

18. Maruyama, M., *et al*. Cerebrospinal fluid amyloid beta(1-42) levels in the mild cognitive impairment stage of Alzheimer's disease. *Exp*. *Neurol*. **172**, 433– 436 (2001).

19. Jack, C.R., Jr., *et al*. Defining imaging biomarker cut points for brain aging and Alzheimer's disease. *Alzheimers Dement*. **13**, 205– 216 (2017).

20. Steenland, K., Zhao, L., Goldstein, F., Cellar, J. & Lah, J. Biomarkers for predicting cognitive decline in those with normal cognition. *J. Alzheimers Dis*. **40**, 587– 594 (2014).

21. Ostrowitzki, S., *et al*. A phase III randomized trial of gantenerumab in prodromal Alzheimer's disease. *Alzheimers Res. Ther*. 2017; **9**, 95 (2017).

22. Villemagne, V.L., *et al*. Amyloid beta deposition, neurodegeneration, and cognitive decline in sporadic Alzheimer's disease: a prospective cohort study. *Lancet Neurol*. **12**, 357– 367 (2013).

23. Villemagne, V.L., *et al.* Longitudinal assessment of Aβ and cognition in aging and Alzheimer disease. *Ann. Neurol*. **69**, 181– 192 (2011).

24. Villain, N., *et al*. Regional dynamics of amyloid-β deposition in healthy elderly, mild cognitive impairment and Alzheimer's disease: a voxelwise PiB-PET longitudinal study. *Brain* **135**, 2126– 2139 (2012).

25. Landau, S.M., *et al*. Measurement of longitudinal β-amyloid change with 18F-florbetapir PET and standardized uptake value ratios. *J. Nucl. Med*. **56**, 567– 574 (2015).

26. Salloway, S., *et al*. Amyloid positron emission tomography and cerebrospinal fluid results from a crenezumab anti-amyloid-beta antibody double-blind, placebo-controlled, randomized phase II study in mild-to-moderate Alzheimer's disease (BLAZE). *Alzheimers Res. Ther*. **10**, 96 (2018).

27. Honig, L.S., *et al*. Trial of solanezumab for mild dementia due to Alzheimer's disease. *N. Engl. J. Med*. 2018; **378**, 321– 330 (2018).

28. Sevigny, J*., et al*. The antibody aducanumab reduces Aβ plaques in Alzheimer's disease. *Nature* **537**, 50– 56 (2016).

29. Klein, G., *et al*. Gantenerumab reduces amyloid-β plaques in patients with prodromal to moderate Alzheimer's disease: A PET substudy interim analysis. *Alzheimers Res. Ther*. **11**, 101 (2019).

30. Ultsch, M., *et al*. Structure of crenezumab complex with Aβ shows loss of β-hairpin. *Sci. Rep*. **6**, 39374 (2016).

31. Bohrmann, B., *et al*. Gantenerumab: A novel human anti-Aβ antibody demonstrates sustained cerebral amyloid-β binding and elicits cell-mediated removal of human amyloid-β. *J. Alzheimers Dis*. 2012 **28**, 49– 69 (2012).

32. Crespi, G.A., Hermans, S.J., Parker, M.W. & Miles, L.A. Molecular basis for mid-region amyloid-β capture by leading Alzheimer's disease immunotherapies. *Sci*. *Rep*. **5**, 9649 (2015).

33. Meilandt, W.J., *et al*. Characterization of the selective in vitro and in vivo binding properties of crenezumab to oligomeric Aβ. *Alzheimers Res. Ther*. **11**, 97 (2019).

34. Belloy, M.E., Napolioni, V. & Greicius, M.D. A Quarter Century of APOE and Alzheimer's Disease: Progress to Date and the Path Forward. *Neuron*. 2019; **101**, 820– 838.

35. Mahley, R.W. Central Nervous System Lipoproteins: ApoE and Regulation of Cholesterol Metabolism. *Arterioscler*. *Thromb*. *Vasc*. *Biol*. **36**, 1305– 1315 (2016).

36. Castellano, J.M., *et al*. Low-density lipoprotein receptor overexpression enhances the rate of brain-to-blood Aβ clearance in a mouse model of β-amyloidosis. *Proc*. *Natl*. *Acad*. *Sci*. *USA*. **109**, 15502– 15507 (2012).

37. Verghese, P.B., *et al*. ApoE influences amyloid-β (Aβ) clearance despite minimal apoE/Aβ association in physiological conditions. *Proc. Natl. Acad. Sci. USA*. **110**, E1807– E1816 (2013).

38. Stockley, J.H., Ravid, R. & O'Neill, C. Altered beta-secretase enzyme kinetics and levels of both BACE1 and BACE2 in the Alzheimer's disease brain. *FEBS Lett.* **580**, 6550– 6560 (2006).

39. Deane, R., *et al*. apoE isoform-specific disruption of amyloid beta peptide clearance from mouse brain. *J. Clin. Invest.* **118**, 4002– 4013 (2008).

40. Yoshida, K., *et al*. Pharmacokinetics and pharmacodynamic effect of crenezumab on plasma and cerebrospinal fluid beta-amyloid in patients with mild-to-moderate Alzheimer's disease. *Alzheimers Res. Ther.* **12**, 16 (2020).

41. Kaschka, W.P., Theilkaes, L., Eickhoff, K. & Skvaril, F. Disproportionate elevation of the immunoglobulin G1 concentration in cerebrospinal fluids of patients with multiple sclerosis. *Infect. Immun.* **26**, 933– 941 (1979).

42. Ovod, V., *et al*. Amyloid β concentrations and stable isotope labeling kinetics of human plasma specific to central nervous system amyloidosis. *Alzheimers Dement*. **13**, 841– 849 (2017).

43. Roberts, K.F., *et al*. Amyloid-β efflux from the central nervous system into the plasma. *Ann. Neurol*. **76**, 837– 844 (2014).

44. Maruyama, M., *et al*. Cerebrospinal fluid neprilysin is reduced in prodromal Alzheimer's disease. *Ann. Neurol*. **57**, 832– 842 (2005).

45. Haeberlein, S.B., *et al*. Aducanumab 36-month data from PRIME: a randomized, double-blind, placebo-controlled Phase 1b study in patients with prodromal or mild Alzheimer's disease. *Neurology.* **90**, S2.004 (2018).

46. Bruhns, P. Properties of mouse and human IgG receptors and their contribution to disease models. *Blood.* **119**, 5640– 5649 (2012).

47. Fleisher, A.S., *et al*. Apolipoprotein E ε4 and age effects on florbetapir positron emission tomography in healthy aging and Alzheimer disease. *Neurobiol. Aging.* **34**, 1– 12 (2013).

48. Sumner, I.L., Edwards, R.A., Asuni, A.A. & Teeling, J.L. Antibody Engineering for Optimized Immunotherapy in Alzheimer's Disease. *Front*. *Neurosci*. **12**, 254 (2018).

49. Fuller, J.P., Stavenhagen, J.B. & Teeling, J.L. New roles for Fc receptors in neurodegeneration–the impact on Immunotherapy for Alzheimer's disease. *Front*. *Neurosci*. **8**, 235 (2014).

50. Guo, Z., *et al*. Apolipoprotein E genotypes and the incidence of Alzheimer's disease among persons aged 75 years and older: variation by use of antihypertensive medication? *Am*. *J. Epidemiol.* **153**, 225– 231 (2001).

Figure Legends

Figure 1 Key pathways for amyloid transport. Aβ, amyloid beta; APP, amyloid precursor protein; BBB, blood–brain barrier; CSF, cerebrospinal fluid.

Figure 2 Calibration and simulation results for plasma PK (A-C), CSF and brain PK (D-F), plasma and CSF PD (G-I), and brain PD (J-L). Aβ, amyloid beta; CSF, cerebrospinal fluid; ISF, interstitial fluid; IV, intravenous; mAb, monoclonal antibody; PD, pharmacodynamic; PK, pharmacokinetic; Q4W, every 4 weeks; SC, subcutaneous; SD, standard deviation.

Figure 3 Model calibrations (A-B) and predictions (C-D) overlaid on observed clinical data of changes in Aβ PET SUVR upon treatment with candidate mAbs: aducanumab Phase Ib PRIME study (A), crenezumab Phase III CREAD and CREAD2 (B), aducanumab Phase III EMERGE study (C), and gantenerumab Phase III SCarlet RoAD and Marguerite RoAD (D). Q4W, every 4 weeks; SC, subcutaneous; SUVR, standard uptake value ratio. [a]Reported in Centiloids.

Figure 4 APOE ε4 carrier and non-carrier predictions for Aβ SUVR. Aβ, amyloid beta; APOE, apolipoprotein E; SUVR, standard uptake value ratio; VP, virtual patient.

SUPPORTING INFORMATION

Additional supporting information may be found in the online version of the article at the publisher's website.

Table 1 Aβ42 biomarker and Aβ SUVR values for normal, prodromal, and moderate-to-severe patients used to guide virtual patient development. Values are mean ± standard deviation unless otherwise specified

Stage	Cognitive impairment	Aβ42 CSF pg/mL	Aβ PET SUVR (PiB tracer)[a]	References
Normal healthy	None	206 ± 55[16] Median = 111 (25–1060)[17] 563.3 ± 191.0[18]	< 1.42[19] (determined as cutoff for Aβ+) typical range 1.17–1.37[19]	Shaw et al. 2009[16] Jack et al. 2017[19] Mehta et al. 2000[17] Maruyama et al. 2001[18]
Prodromal	Early mild/ mild	≤ 192[20] 146 ± 38[16] 539.5 ± 149.6[18] (focus on intra-study values for trend)	1.65[21] Rate of increase of .043 in SUVR (~3%)/year[22-24] Rate of increase 1.3%/year[25]	Steenland et al. 2014[20] Shaw et al. 2009[16] Ostrowitzki et al. 2017[21] Villemagne et al. 2013[22] Villemagne et al. 2011[23] Villain et al. 2012[24] Maruyama et al. 2001[18] Landau et al. 2015[25]
AD	Dementia	144 ± 41[16] Median = 38 (25–325)[16] 397.6 ± 164.1[18]	~1.8–2.0 (mild to moderate AD)[26] ~2.2 and greater (severe)[22] Rate of increase slows in late stages[22-24]	Shaw et al. 2009[16] Salloway et al. 2018[26] Villemagne et al 2013[22] Villemagne et al. 2011[23] Villain et al. 2012[24] Mehta et al. 2000[17] Maruyama et al. 2001[18]

[a]Cortical SUVR with cerebellar cortex reference region.

Aβ, amyloid beta; AD, Alzheimer's disease; CSF, cerebrospinal fluid; PET, positron emission tomography; PiB, Pittsburgh Compound B; SUVR, standard uptake value ratio.

Table 2 Antibody (mAb) dissociation constants for Aβ monomers, oligomers, fibrils, and plaque

mAb	K_D Monomers	K_D Oligomers	K_D Fibril/plaque	References
Crenezumab	3-5 nM[30]	0.4-0.6 nM[30]	50 nM[a]	Ultsch et al. 2016[30]
Gantenerumab	17 nM	1.2 nM	0.6 nM	Bohrmann et al. 2012[31]
Solanezumab	10 pM[b]	0	0	Crespi et al. 2015[32]
Aducanumab	> 1 μM	0.1 nM	0.1 nM	Sevigny et al. 2016[28]

[a]Assumption used because crenezumab binds plaque poorly relative to oligomers.[33]

[b]Estimated from Crespi et al. 2015.[32]

Aβ, amyloid beta; K_D, equilibrium dissociation constant; mAb, monoclonal antibody.

Table 3 Mechanistic differences in *APOE ε4* carriers and non-carriers in the literature

Parameter	*APOE ε4*+ VP Value	*APOE ε4*- VP Value	Reference
BACE1 K_m (μM)	7.760	8.438	Stockley et al. 2006[38]
BACE1 V_{max} (μM/h)	0.455	0.253	Stockley et al. 2006[38]
Aβ40 astrocyte receptor clearance fraction	0.100	0.200	Deane et al. 2008[39]
Aβ42 astrocyte receptor clearance fraction	0.117	0.235	Deane et al. 2008[39]
Aβ40 brain to CSF clearance fraction	0.301	0.602	Deane et al. 2008[39]
Aβ42 brain to CSF clearance fraction	0.353	0.707	Deane et al. 2008[39]
Aβ40 brain to plasma active clearance fraction	0.349	0.698	Deane et al. 2008[39]
Aβ42 brain to plasma active clearance fraction	0.246	0.492	Deane et al. 2008[39]

Clearance fraction parameters are expressed in terms of the fraction of clearance attributed to each pathway for the *APOE ε4*+ VP. Fractions add up to > 1 for *APOE ε4*- VP, indicating that the total clearance is expected to increase. Aβ40 and Aβ42 refer to Aβ monomers.

Aβ, amyloid beta; APOE, apolipoprotein E; BACE1, beta-secretase 1; CSF, cerebrospinal fluid; K_m, enzyme concentration at half of V_{max}; V_{max}, maximum rate of reaction; VP, virtual patient.

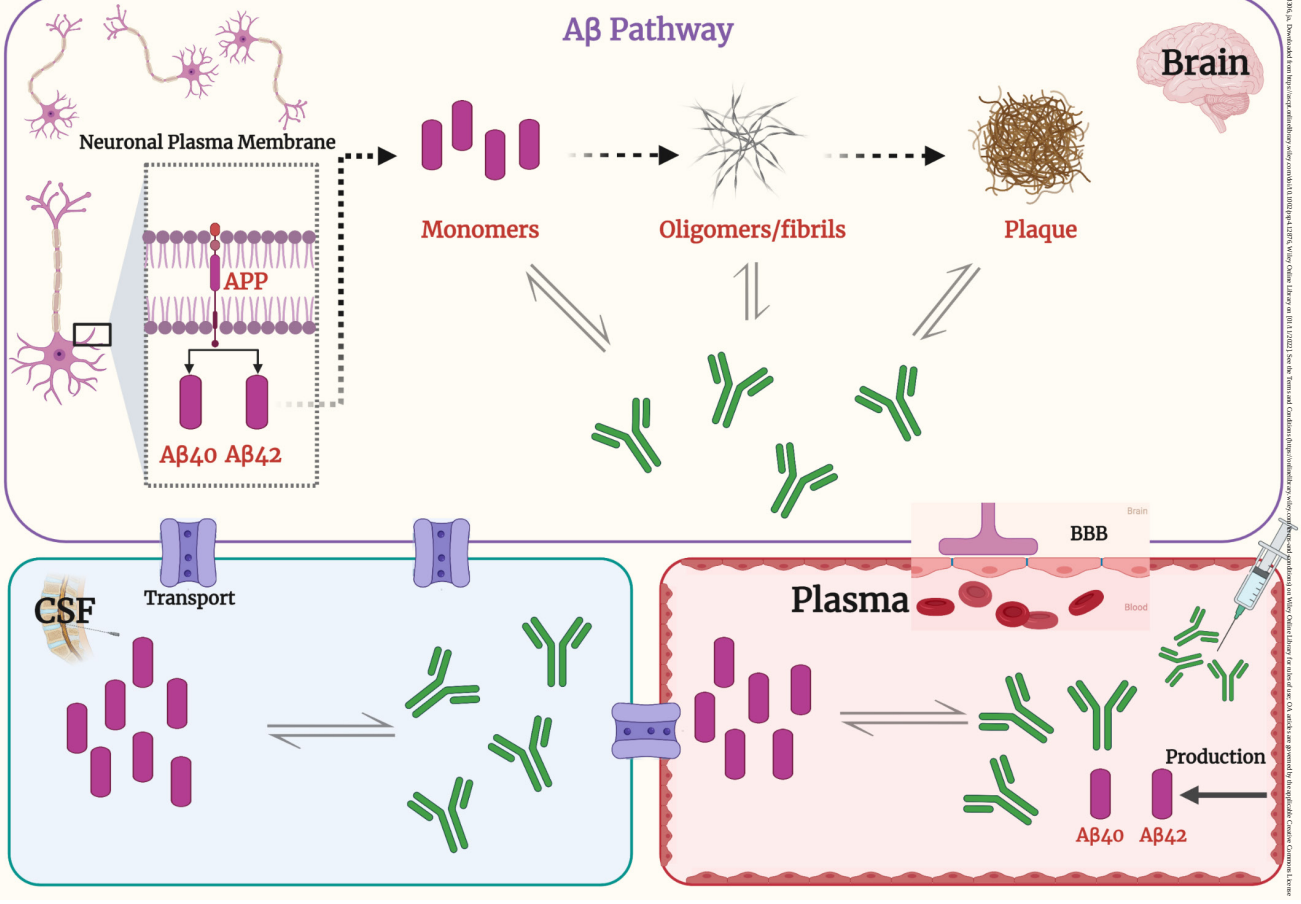
Aβ Pathway
Brain
Neuronal Plasma Membrane
APP
Aβ40 Aβ42
Monomers
Oligomers/fibrils
Plaque
CSF
Transport
BBB
Brain
Blood
Plasma
Production
Aβ40 Aβ42

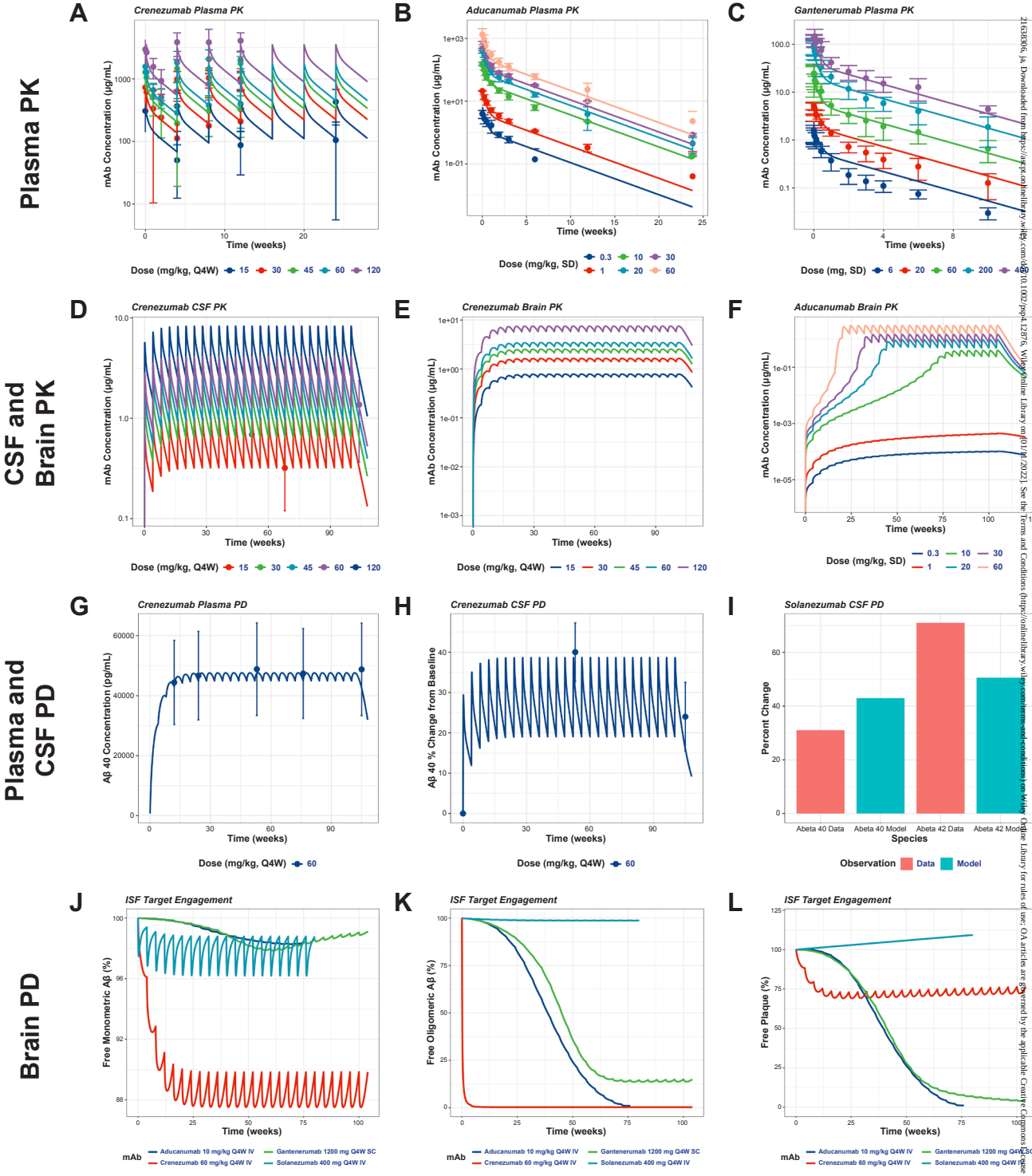

Calibration

Prediction